Hindawi
Mathematical Problems in Engineering
Volume 2019, Article ID 5759427, 8 pages
https://doi.org/10.1155/2019/5759427

Research Article

Efficient Localization Algorithm for Near-Field Noncircular Sources via Dual-Polarization Sensor Array

Jiaqi Song and Haihong Tao

National Laboratory of Radar Signal Processing, Xidian University, Xi'an 710071, China

Correspondence should be addressed to Haihong Tao; hhtao@xidian.edu.cn

Received 29 July 2019; Accepted 27 November 2019; Published 12 December 2019

Academic Editor: Fazal M. Mahomed

Noncircular signals are widely used in the area of radar, sonar, and wireless communication array systems, which can offer more accurate estimates and detect more sources. In this paper, the noncircular signals are employed to improve source localization accuracy and identifiability. Firstly, an extended real-valued covariance matrix is constructed to transform complex-valued computation into real-valued computation. Based on the property of noncircular signals and symmetric uniform linear array (SULA) which consist of dual-polarization sensors, the array steering vectors can be separated into the source position parameters and the nuisance parameter. Therefore, the rank reduction (RARE) estimators are adopted to estimate the source localization parameters in sequence. By utilizing polarization information of sources and real-valued computation, the maximum number of resolvable sources, estimation accuracy, and resolution can be improved. Numerical simulations demonstrate that the proposed method outperforms the existing methods in both resolution and estimation accuracy.

1. Introduction

Passive source localization is a key problem in array signal processing for applications such as radar, sonar, microphone arrays, and communication [1]. In recent years, it has received more concern and has developed lots of methods to deal with this issue. Among them, the most typical algorithms are multiple signal classification (MUSIC) [2], estimating signal parameter via rotational invariance techniques (ESPRIT) [3], and their derivatives. Nevertheless, these methods are under the assumption that the sources are in the far-field (FF), which means the wavefronts are plane waves and therefore only direction-of-arrival (DOA) parameters are required to be estimated.

However, when the radiating sources are located in the near-field (NF) of the array, whose wavefronts are spherical waves, both DOA and range parameters should be estimated to localize the sources. Thus, the traditional FF algorithms are no longer suitable for NF sources. Fortunately, many advanced algorithms have been presented under NF assumption. Huang and Barkat proposed a two-dimensional (2-D) MUSIC method in the angle-range domain to achieve NF super-resolution localization, but the 2-D joint search brought high computational complexity [4]. Challa and Shamsunder took the lead in introducing high-order cumulant into NF source parameter estimation problem. By constructing multiple cumulant matrixes, they proposed ESPRIT-Like to estimate DOA and range parameters of NF sources [5]. However, the ESPRIT-Like algorithm had many drawbacks, such as high computational complexity, parameter pairing, and array aperture loss. Lee et al. proposed a covariance approximation method (CA) [6]. The method reconstructed the elements of the NF covariance matrix, so that the NF source was converted into a virtual FF source (the DOA information was the same), and the traditional FF direction finding methods could apply to the DOA estimation of FF sources, avoiding multidimensional search. But the CA algorithm would produce an image source in the case of coherent sources. Noh and Lee analyzed the phenomenon and proposed a method to suppress the image source effectively [7]. Grosicki et al. proposed the weighted linear prediction (WLP) algorithm to obtain the DOA and

range estimation [8]. Utilizing the symmetric linear array, Zhi and Chia proposed the classical generalized ESPRIT algorithm [9].

In recent years, many direction-finding methods which employ the noncircular signals received more concern, such as Binary Phase Shift Keying (BPSK), Pulse Amplitude Modulation (PAM), and Amplitude Shift Keying (ASK) signals. By taking use of the noncircularity of the signal, the array can benefit from the extended virtual aperture, which means that the resolution capability and the estimation accuracy can be improved. Chen et al. considered the DOA estimation of noncircular signal for uniform linear array via the propagation method and Euler transformation [10]. Tan et al. proposed a weighted unitary nuclear norm minimization approach for DOA estimation in the strictly noncircular sources case [11]. Xie et al. proposed a real-valued localization algorithm for noncircular signals using the uniform linear array [12]. Furthermore, Xie et al. proposed another near-field localization method for noncircular sources via generalized ESPRIT [13]. Chen et al. proposed a novel localization method for NF rectilinear or strictly noncircular sources with a symmetric uniform linear array of cocentered orthogonal loop and dipole (COLD) antennas [14].

However, most of the abovementioned algorithms use the scalar sensors array, which cannot exploit the polarization information embedded in the electromagnetic waves. An array of vectors sensors can detect signals by utilizing the polarization diversity. For this reason, electromagnetic vector sensors array signal processing has attracted much attention in recent years. Obeidat et al. proposed polarization ESPRIT-Like algorithm by using polarization sensitive array [15]. However, it suffers from half aperture loss. To avoid the aperture loss problem, Wu et al. developed a least squares-virtual ESPRIT algorithm (LS-VESPA) [16]. But it involves extra parameter pairing procedure. Based on the symmetric sparse linear array with dual-polarization sensors, Tao et al. proposed the Fresnel-region rank reduction (FR-RARA) algorithm [17] that enhanced array aperture and only required second-order statistics. He et al. presented a NF localization of partially polarization sources with a cross-dipole array [18].

In this paper, we construct an augmented covariance matrix which consists of the real part and imaginary part of array outputs data. Then, based on the noncircularity of signals and the property of symmetric uniform linear array (SULA), the array steering vector could be decoupled as the product of three real-valued matrixes including DOA, range, and other nuisance parameters, respectively. Consequently, a rank reduction- (RARE-) based localization method is derived, which translates multidimensional spectral search into multiple one-dimensional (1-D) spectral searches. The proposed method has the following advantages: (1) As a result of the exploitation of non-circularity, more sources can be resolved. (2) It is efficient since it avoids exhaustive complex-valued computation and multidimensional search. (3) The estimation accuracy and resolution are improved effectively by utilizing the noncircularity and polarization diversity.

The rest of this paper is organized as follows. In Section 2, the data model for NF noncircular signals which received by dual-polarization sensors SULA is formulated. The proposed localization algorithm for NF noncircular sources is developed in Section 3. In Section 4, we discuss the performance of the proposed algorithm and some newly developed algorithms. Then, numerical simulations are presented in Section 5. Conclusion is drawn in Section 6.

Notations: The transpose, conjugate, and conjugate transpose are denoted by, $(\cdot)^*$, and $(\cdot)^H$, respectively. The symbol $\otimes$ represents the Kronecker product. $\Re(\cdot)$, $\Im(\cdot)$, and $\det(\cdot)$ symbolize the real part operator, the imaginary part operator, and the determinant of a matrix.

2. Signal Model

We suppose that K independent NF noncircular signals impinge upon a SULA as shown in Figure 1. The array is composed of $N = 2M + 1$ dual-polarization sensors which is placed along the y-axis, and its sensors position is $[-M\,d, \ldots, 0, \ldots, M\,d]$, where d is the interelement spacing. The dual-polarization sensors used in this paper is cross-dipole. This localization algorithm is achievable by other polarization sensors, such as cocentered orthogonal loop and dipole pair [19]. But the cross-dipole is very small and easier to design, so it is more common in practice.

Note that the two polarization components of the cross-dipole point to the x-axis and y-axis directions, respectively. Assuming that all sources are located in the y-z plane, then the two direction components of electronic field can be described as

$$\mathbf{E} = \begin{bmatrix} e_x \\ e_y \end{bmatrix} = \begin{bmatrix} -\cos(\alpha) \\ \cos(\theta)\sin(\alpha)e^{j\beta} \end{bmatrix}, \tag{1}$$

where α denotes the auxiliary polarization angle, β represents the polarization phase difference, and θ signifies the DOA of the signal.

Let the array center (sensor 0) be the reference point; the output signal components in x-polarization and y-polarization received by the mth sensor at time t can be modeled as

$$u_m^{[x]} = -\sum_{k=1}^{K} s_k(t)e^{j\tau_{mk}}\cos(\alpha_k) + n_m^{[x]}, \tag{2}$$

$$u_m^{[y]} = \sum_{k=1}^{K} s_k(t)e^{j\tau_{mk}}\cos(\theta_k)\sin(\alpha_k)e^{j\beta_k} + n_m^{[y]}, \tag{3}$$

where $s_k(t)$ denotes the kth signal, $k = 1, \ldots, K$, τ_{mk} represents the phase shift related to the kth signal's propagation time delay from the reference point to the mth sensor, α_k, β_k, and θ_k are the auxiliary polarization angle, polarization phase difference, and DOA of kth signal, and $n_m^{[x]}$ and $n_m^{[y]}$ symbolize the additive noise.

Consider that the sources are located in the NF, the time delay τ_{mk} can be approximated as [4]

$$\tau_{mk} = m\omega_k + m^2\phi_k, \tag{4}$$

where $\omega_k = -2\pi d\sin(\theta_k)/\lambda$, $\phi_k = \pi d^2\cos^2\theta_k/\lambda r_k$, λ denotes the wavelength of signal, and r_k represents the range parameter of the kth source.

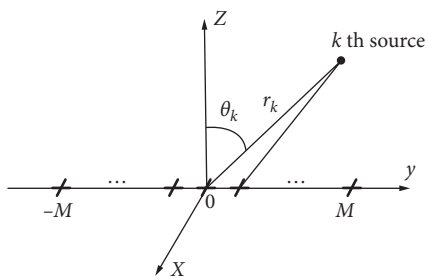

Figure 1: Symmetric uniform linear array with dual-polarization sensors.

When the source signals are noncircular signals, it can be obtained that $s_k(t) = e^{j\psi_k} s_{0,k}(t)$; herein, $\{\psi_k\colon k = 1, \ldots, K\}$ is the noncircular phase of the kth signals and $s_{0,k}(t)$ is the zero-phased version of the source signal.

In a matrix form, (2) and (3) can be written as

$$\mathbf{u}(t) = \mathbf{A}\mathbf{s}(t) + \mathbf{n}(t), \tag{5}$$

where

$$\begin{aligned}
\mathbf{u}(t) &= \left[\, \mathbf{u}^{[x]}(t) \;\; \mathbf{u}^{[y]}(t) \,\right]^T \\
\mathbf{u}^{[x]}(t) &= \left[\, u_{-M}^{[x]} \;\cdots\; u_0^{[x]} \;\cdots\; u_M^{[x]} \,\right], \\
\mathbf{u}^{[y]}(t) &= \left[\, u_{-M}^{[y]} \;\cdots\; u_0^{[y]} \;\cdots\; u_M^{[y]} \,\right], \\
\mathbf{A} &= \left[\, \mathbf{a}_1 \;\; \mathbf{a}_2 \;\cdots\; \mathbf{a}_K \,\right], \\
\mathbf{s}(t) &= \left[\, s_1(t) \;\; s_2(t) \;\cdots\; s_K(t) \,\right]^T, \\
\mathbf{n}(t) &= \left[\, \mathbf{n}^{[x]}(t) \;\; \mathbf{n}^{[y]}(t) \,\right]^T.
\end{aligned} \tag{6}$$

In the above equations, $\mathbf{u}(t)$ is array output vector, $\mathbf{A}$ represents the array steering matrix, $\mathbf{s}(t)$ symbolizes the source signal vector, and $\mathbf{n}(t)$ denotes the additive noise matrix.

With a total of L snapshots taken at the distinct instants $\{t_l\colon l = 1, \ldots, L\}$, the problem is to determine the localization parameters from the array output data. Throughout this paper, the following hypotheses are assumed to hold:

(1) The incoming signals are mutually independent, narrowband stationary noncircular

(2) The sensor noise is additive zero-mean white Gaussian and independent of the source signals

(3) In order to avoid the phase ambiguity, the intersensor spacing d should be within a quarter wavelength

(4) The range parameter r lies in $[0.62\sqrt{D^3/\lambda}, 2D^2/\lambda]$ which means the signal sources lies in the NF [20], where D is the aperture of array

3. Proposed Algorithm

The traditional subspace estimation algorithm requires multidimensional spectral peak search that exhausts high computational burden. And to the best of our knowledge, there has been very limited work utilizing polarization diversity and the noncircularity of signals simultaneously. In order to overcome these shortages and improve estimation performance, we construct a real-valued augmented output matrix based on the Euler equation. Then, the steering vector is factorized with respect to the localization parameters and nuisance parameters. Based on the RARE criterion [21] and 1-D search, the localization parameters can be estimated. Consequently, the multidimensional optimization problem could be accomplished by real-valued computation and 1-D spectral searches.

3.1. Real-Valued Augmented Covariance Matrix. In order to transform the complex-valued data into real-valued domain, we achieve the real part and imaginary part of $\mathbf{x}(t)$, respectively, by the following equations:

$$\begin{aligned}
\Re[\mathbf{x}(t)] &= \frac{[\mathbf{x}(t) + \mathbf{x}^*(t)]}{2}, \\
\Im[\mathbf{x}(t)] &= \frac{[\mathbf{x}(t) - \mathbf{x}^*(t)]}{2j}.
\end{aligned} \tag{7}$$

According to the signal model in (5), we can construct the real-valued augmented data matrix as

$$\mathbf{Y}(t) = \begin{bmatrix} \Re\mathbf{u}^{[x]}(t) \\ \Im\mathbf{u}^{[x]}(t) \\ \Re\mathbf{u}^{[y]}(t) \\ \Im\mathbf{u}^{[y]}(t) \end{bmatrix} = \mathbf{A}_r\mathbf{s}(t) + \mathbf{n}_r(t), \tag{8}$$

where $\mathbf{A}_r$ is the augmented steering matrix and $\mathbf{n}_r$ is the augmented noise matrix. And the th row of $\mathbf{A}_r$ can be expressed as

$$\mathbf{a}_r(\theta_k, r_k) = \left[\mathbf{a}_{ck}^{[x]}, \mathbf{a}_{sk}^{[x]}, \mathbf{a}_{ck}^{[y]}, \mathbf{a}_{sk}^{[y]}\right]^T. \tag{9}$$

The elements in $\mathbf{a}_r(\theta_k, r_k)$ is formulated in (10), where $m = -M, \ldots, 0, \ldots, M$:

$$\begin{aligned}
\mathbf{a}_{ck}^{[x]} &= \left[-\cos(\alpha_k)\cos\left(m\omega_k + m^2\phi_k + \psi_k\right)\right]_{1\times(2M+1)}, \\
\mathbf{a}_{ck}^{[y]} &= \left[-\cos(\alpha_k)\sin\left(m\omega_k + m^2\phi_k + \psi_k\right)\right]_{1\times(2M+1)}, \\
\mathbf{a}_{ck}^{[x]} &= \left[\cos(\theta_k)\sin(\alpha_k)\cos\left(m\omega_k + m^2\phi_k + \beta_k + \psi_k\right)\right]_{1\times(2M+1)}, \\
\mathbf{a}_{ck}^{[y]} &= \left[\cos(\theta_k)\sin(\alpha_k)\sin\left(m\omega_k + m^2\phi_k + \beta_k + \psi_k\right)\right]_{1\times(2M+1)}.
\end{aligned} \tag{10}$$

Then, the real-valued augmented covariance matrix of $\mathbf{Y}(t)$ can be expressed as $\mathbf{R} = E[\mathbf{Y}(t)\mathbf{Y}^H(t)]$. By taking the eigen-decomposition (EVD) of $\mathbf{R}$, we have

$$\mathbf{R} = \mathbf{U}_s\mathbf{\Lambda}_s\mathbf{U}_s^H + \mathbf{N}_s\mathbf{\Lambda}_n\mathbf{N}_s^H, \tag{11}$$

where $\mathbf{\Lambda}_s$ and $\mathbf{\Lambda}_n$ are the diagonal matrixes which contain K largest eigenvalues and other $4N - K$ smallest eigenvalues. $\mathbf{U}_s$ is a $4N \times K$ matrix spanning the signal subspace of $\mathbf{R}$, and $\mathbf{U}_n$ is a $4N \times (4N - K)$ matrix spanning the noise subspace of $\mathbf{R}$,

3.2. Joint DOA, Range, and Polarization Estimation. According to the principle of MUSIC, the parameters can be estimated by multidimensional searching of the following spectrum function:

$$P = \mathbf{a}^H(\theta, r)\mathbf{U}_n\mathbf{U}_n^H\mathbf{a}(\theta, r). \tag{12}$$

It is obvious that K sets of parameters can be achieved by finding the K minimum value of $P(\theta, r)$. However, the estimator in (12) is computationally intensive since it requires 2-D spectral search. To avoid the high-dimensional computation, the augmented steering vector can be factorized, leading to a simple 1-D operation.

Due to the symmetric property of array steering vector, the augmented steering vector can be decoupled as the following formation:

$$\mathbf{a}(\theta, r) = \mathbf{V}(\theta)\mathbf{F}(\theta, r)\mathbf{g}, \tag{13}$$

where

$$\begin{aligned} \mathbf{V}(\theta) &= \mathbf{I}_{2\times 2} \otimes \begin{bmatrix} \mathbf{V}_1 & -\mathbf{V}_2 \\ \mathbf{V}_2 & \mathbf{V}_1 \end{bmatrix}, \\ \mathbf{F}(\theta, r) &= \mathbf{I}_{2\times 2} \otimes \begin{bmatrix} \mathbf{f}_1 & -\mathbf{f}_2 \\ \mathbf{f}_2 & \mathbf{f}_1 \end{bmatrix}. \end{aligned} \tag{14}$$

Herein,

$$\mathbf{V}_1 = \begin{bmatrix} \cos(-M\omega_k) & & & & \\ & \cos(-(M-1)\omega_k) & & & \\ & & \cdots & & \\ & & & 1 & \\ & & \cdots & & \\ & \cos((M-1)\omega_k) & & & \\ \cos(M\omega_k) & & & & \end{bmatrix}_{(2M+1)\times(M+1)}, \tag{15}$$

$$\mathbf{V}_2 = \begin{bmatrix} \sin(-M\omega_k) & & & & \\ & \sin(-(M-1)\omega_k) & & & \\ & & \cdots & & \\ & & & 0 & \\ & & \cdots & & \\ & \sin((M-1)\omega_k) & & & \\ \sin(M\omega_k) & & & & \end{bmatrix}_{(2M+1)\times(M+1)}, \tag{16}$$

$$\mathbf{f}_1 = \begin{bmatrix} \cos(M^2\phi_k) & \cos\left((M-1)^2\phi_k\right) & \cdots & 1 \end{bmatrix}^T_{(M+1)\times 1}, \tag{17}$$

$$\mathbf{f}_2 = \begin{bmatrix} \sin(M^2\phi_k) & \sin\left((M-1)^2\phi_k\right) & \cdots & 0 \end{bmatrix}^T_{(M+1)\times 1}, \tag{18}$$

$$\mathbf{g} = \begin{bmatrix} -\cos(\alpha_k)\cos(\psi_k) \\ -\cos(\alpha_k)\sin(\psi_k) \\ \sin(\alpha_k)\cos(\theta_k)\cos(\psi_k + \beta_k) \\ \sin(\alpha_k)\cos(\theta_k)\sin(\psi_k + \beta_k) \end{bmatrix}. \tag{19}$$

If and only if $(\theta, r) = (\theta_k, r_k)$, $k = 1, \ldots, K$, the following equation holds:

$$\mathbf{a}^H(\theta, r)\mathbf{U}_n\mathbf{U}_n^H\mathbf{a}(\theta, r) = 0. \tag{20}$$

Equation (20) can be rewritten as

$$\mathbf{Q}^H(\theta, r)\mathbf{C}_1(\theta)\mathbf{Q}(\theta, r) = 0. \tag{21}$$

where $\mathbf{Q}(\theta, r) = \mathbf{F}(\theta, r)\mathbf{g}$ and $\mathbf{C}_1(\theta) = \mathbf{V}^H(\theta)\mathbf{U}_n\mathbf{U}_n^H\mathbf{V}(\theta)$.

It is noteworthy that $\mathbf{C}_1$ is only related to θ and independent with other parameters. Since $\mathbf{C}_1(\theta) = \mathbf{V}^H(\theta)\mathbf{U}_n\mathbf{U}_n^H\mathbf{V}(\theta)$ and $\mathbf{V}(\theta) \in \mathbf{R}^{4(2M+1)\times 4(M+1)}$, $\mathbf{U}_n \in \mathbf{R}^{4(2M+1)\times[4(2M+1)-K]}$, so if $4(2M+1) - K \geq 4(M+1)$ (i.e., $K \leq 4M$), $\mathbf{C}_1(\theta)$ is generally of full column rank. Thus, only if $\theta = \theta_k$, $k = 1, \ldots, K$, (21) becomes true because the rank of $\mathbf{C}_1(\theta)$ drops according to the RARE criterion. Therefore, the DOAs of sources can be estimated by the following spectrum function:

$$f_1(\theta) = \frac{1}{\det(\mathbf{C}_1(\theta))}. \tag{22}$$

After finding K peaks of $f_1(\theta)$ through a 1-D search, the DOAs of sources are obtained. Therefore, the range parameters of sources can be achieved via another RARE estimator.

Define $\mathbf{C}_2(\theta, r) = \mathbf{F}^H(\theta, r)\mathbf{V}^H(\theta)\mathbf{U}_n\mathbf{U}_n^H\mathbf{V}(\theta)\mathbf{F}(\theta, r)$, then (20) can be expressed as

$$\mathbf{g}^H\mathbf{C}_2(\theta, r)\mathbf{g} = 0. \tag{23}$$

Similarly, since $\mathbf{g} \neq 0$, (23) can hold true if $\mathbf{C}_2(\theta)$ drops rank. Therefore, with obtained $\widehat{\theta}_k$, the range of sources can be estimated by of the following 1-D spectrum searching function for K times:

$$f_2(r) = \frac{1}{\det\left(\mathbf{C}_2(\widehat{\theta}, r)\right)}. \tag{24}$$

3.3. Implementation of the Algorithm. Note that the exact covariance matrix and subspaces are utilized in the previous sections, but the theoretical covariance matrix is unavailable due to the limited snapshots. In practice, it can be estimated as

$$\widehat{R}_Y = \frac{1}{L}\sum_{t=1}^{L}\mathbf{Y}(t)\mathbf{Y}^T(t). \tag{25}$$

To summarize, the procedures of the proposed method are shown as follows:

(1) Reconstruct the real-valued augmented data matrix $\mathbf{Y}(t)$ based on array output matrix and Euler equation.

(2) Take eigen-decomposition operation of the covariance matrix $\mathbf{R}_Y$, and obtain noise subspace matrix $\mathbf{U}_n$.

(3) Compute rank reduction matrix $\mathbf{C}_1$, and estimate DOAs of signals by searching the K highest peaks of (22).

(4) Compute rank reduction matrix $\mathbf{C}_2$, with obtained DOAs $(\widehat{\theta}_k, k = 1, \ldots, K)$ estimate the range parameter $\widehat{r}_k$ by searching the highest peak of (24),

Table 1: Computational complexity of different algorithms.

Method	Matrices	EVDs	Spectral search
GESPRIT	$O(2N^2/L)$	$8N^3/3$	$KN^2/\Delta_r\,(R_{\max}-R_{\min})+360N^2/\Delta_\theta$
FR-RARE	$O(4N^2/L)$	$32N^3/3$	$4KN^2/\Delta_r\,(R_{\max}-R_{\min})+720N^2/\Delta_\theta$
Proposed	$O(4N^2/L)$	$32N^3/3$	$16KN^2/\Delta_r\,(R_{\max}-R_{\min})+2880N^2/\Delta_\theta$

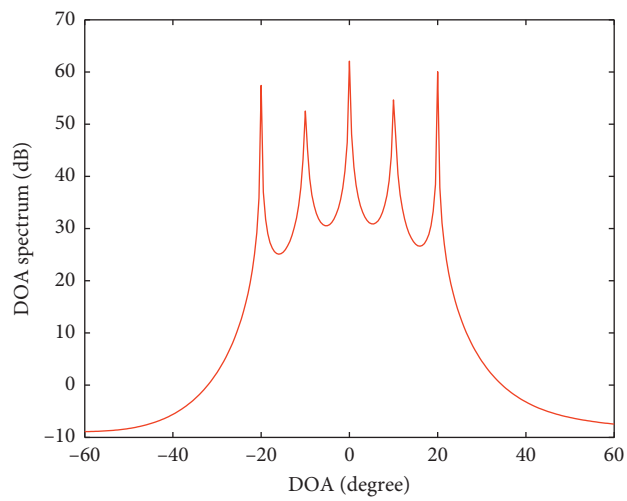

Figure 2: DOA spectrum of the proposed method.

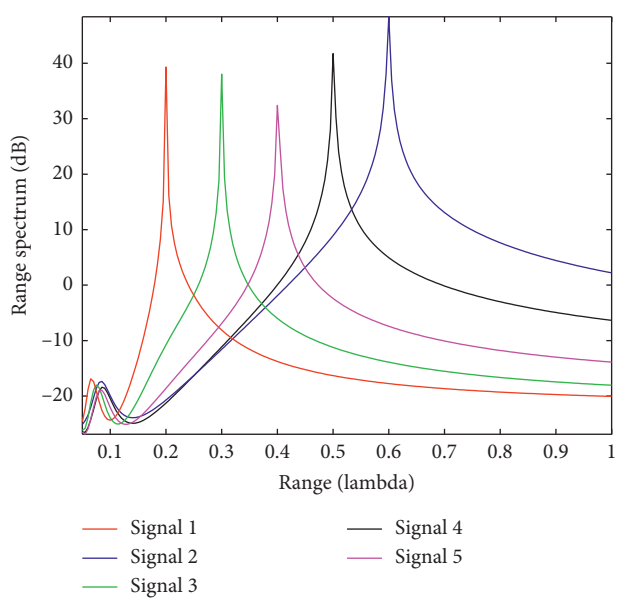

Figure 3: DOA spectrum of the proposed method.

repeat this step from $k = 1$ to K. If the polarization parameters of signals need to be estimated, do step 5.

(5) Decouple the vector $\mathbf{g}$ like (13) further and separate the noncircular parameter from polarization; the polarization can be obtained by another RARE estimator.

(6) Insert estimated $\widehat{\theta}_k$, $\widehat{r}_k$, $\widehat{\alpha}_k$, and $\widehat{\beta}_k$ into (12). By searching the highest peaks of $1/P$, the noncircular parameter is estimated. Repeat this step from $k = 1$ to K.

4. Discussion

4.1. Maximum Number of Resolvable Sources. In this part, we discuss the maximum numbers of resolvable sources of GESPRIT [9], FR-RARE [17], and the proposed method, respectively. To facilitate the analysis, a SULA is assumed to

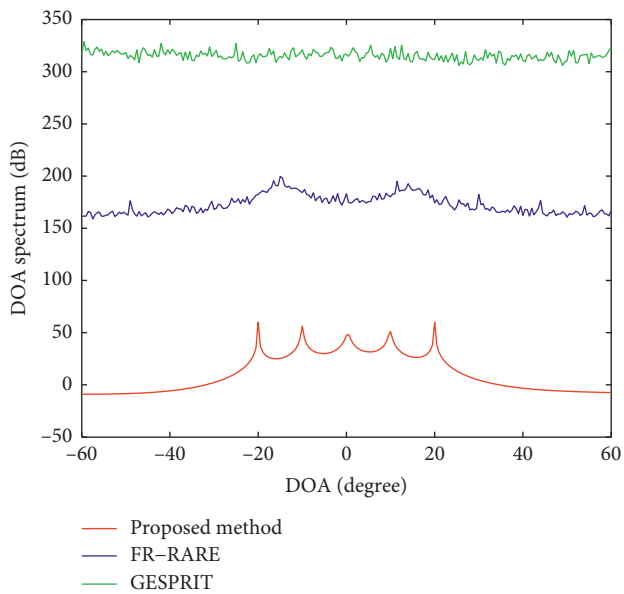

Figure 4: DOA spectrum of the proposed method, FR-RARE and GESPRIT.

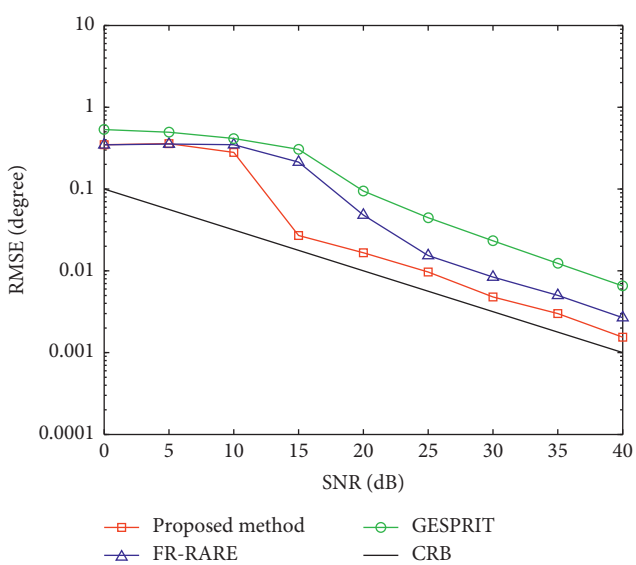

Figure 5: RMSEs of DOA estimates versus SNR.

have $N = 2M + 1$ elements. Since GESPRIT brings half aperture loss, it can handle M sources at most. Because the subspace-based algorithm needs at least one eigenvector to span noise space, FR-RARE can resolve up to $2M$ sources. For the proposed method, the noncircularity has been utilized to construct an extended subspace; hence, it can estimate $4M$ sources at most, which is doubled, compared with FR-RARE.

4.2. Computational Complexity. In this part, only the major computation complexity is considered, such as construction of statistical matrices, eigenvalue decomposition (EVD), and spectral search. The search stepsizes for the angle parameter $\theta \in [-90^\circ, 90^\circ]$ and range parameter $[0.62\sqrt{D^3/\lambda}, 2D^2/\lambda]$ are denoted as Δ_θ and Δ_r. We assume that the number of an array is N and the number of snapshots equals L. The GESPRIT algorithm requires the construction of two $N \times N$ second-order covariance matrices, two EVDs, and twice spectral searches for DOA and range estimation. FR-RARE builds a $2N \times 2N$ second-order covariance matrices, performs the EVD, and twice spectral searches for DOA and range estimation. For the proposed one, it needs to establish a $4N \times 4N$ second-order real-valued covariance matrix, perform EVD on this matrix, and execute 1-D spectral search (Table 1).

5. Numerical Simulation

In this section, numerical simulations are conducted to validate the performance of the proposed algorithm. Without loss of generality, we consider a uniform linear symmetric array composed of 5 dual-polarization sensors ($M = 2$) with the interelement spacing being a quarter-wavelength. The NF signal sources impinged upon the array are equipowered, statistically independent BPSK signal (code rate = 0.1/Ts, noncircularity = 1). Moreover, the estimation performance is measured by the root mean-square error (RMSE) of independent 500 Monte Carlo trials. The RMSE is defined as

$$\mathrm{RMSE} = \sqrt{\frac{1}{500}\sum_{n=1}^{500}\left(\hat{y}_k - y_k\right)^2}, \tag{26}$$

where y_k is the exact DOA θ_k or the range r_k, and $\hat{y}_k$ denotes the estimation of y_k.

In the first experiment, we suppose that five BPSK equipower signals are located at $(-20^\circ, 0.2\lambda, -20^\circ, -20^\circ)$, $(-10^\circ, 0.3\lambda, -10^\circ, -10^\circ)$, $(0^\circ, 0.4\lambda, 0^\circ, 0^\circ)$, $(10^\circ, 0.5\lambda, 10^\circ, 10^\circ)$, and $(20^\circ, 0.6\lambda, 20^\circ, 20^\circ)$, respectively. The snapshot number and signal-to-noise ratio (SNR) are set as 500 and 20 dB. The DOA and range spectrums of proposed method are shown in

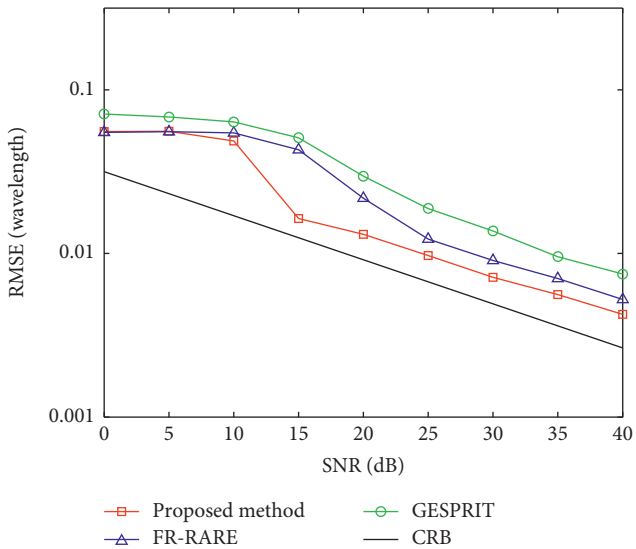

Figure 6: RMSEs of range estimates versus SNR.

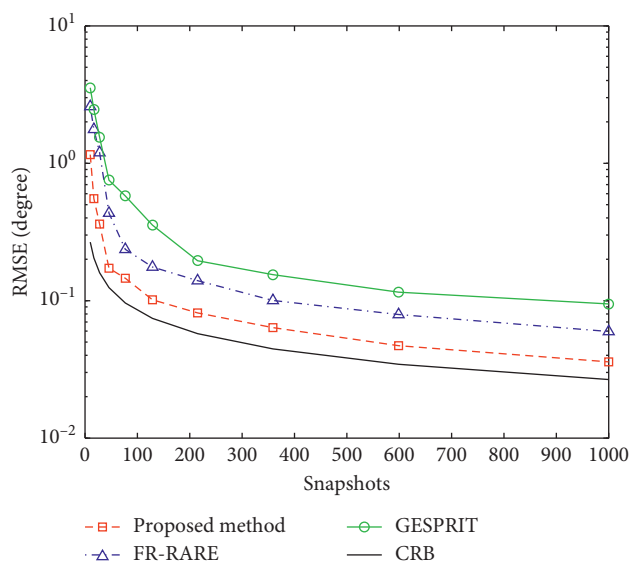

Figure 7: RMSEs of DOA estimates versus snapshots.

Figures 2 and 3. And one can observe that all the sources have been resolved effectively. The DOA spectrums of proposed method, GESPRIT [9], and FR-RARE [17] are plotted in Figure 4. By employing real-valued computations, the proposed method can resolve up to $4M$ sources while FR-RARE can only handle $2M$ sources. Since GESPRIT brings half aperture loss, it can handle M sources at most.

In the second experiment, we investigate RMSEs of the proposed method, GESPRIT and FR-RARE with the variation of SNR. We consider two BPSK signals are located at $(-5^\circ, 1.2\lambda, -5^\circ, -5^\circ)$ and $(2^\circ, 1.8\lambda, 2^\circ, 2^\circ)$. The snapshots number is fixed at 500 and the SNR varies from 0 dB to 40 dB in a stepsize of 5 dB. The RMSEs versus SNR are illustrated in Figures 5 and 6. It is obvious that the estimation performance of two algorithms improves as the SNR increases. Moreover, as a result of higher degrees of freedom (DOFs),

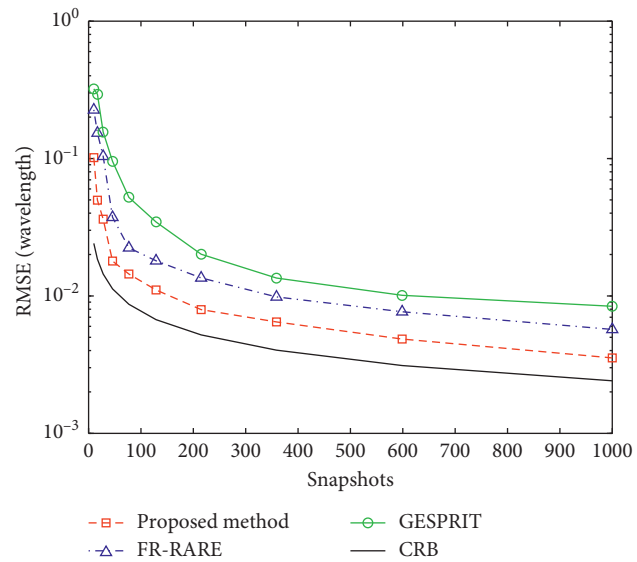

Figure 8: RMSEs of range estimates versus snapshots.

the estimation accuracy of the proposed method is higher than GESPRIT and FR-RARE. Furthermore, there is a significant improvement of algorithm performance when the two sources are close to each other, which means the resolution of the proposed method is higher.

In the third experiment, we study the estimation performance with the variation of snapshots. The parameter settings of two signals are the same as that of the second experiment. The SNR is set to 20 dB, and the number of snapshots varies from 1 to 1000. Figures 7 and 8 leads to a similar conclusion as in the second experiment that the RMSEs decrease with the increasing number of snapshots. This is because that larger samples will provide a better estimate of the covariance matrix for stationary data.

6. Conclusion

In this paper, a novel localization algorithm for the near-field noncircular signals is presented by employing the real-valued computation and 1-D search. The proposed method utilizes the polarization information and noncircularity, which improves the estimation performance significantly. Compared with some existing works, the proposed method has achieved more resolvable signals and improved estimation accuracy and resolution. The simulation results demonstrate the efficiency and effectiveness of the proposed method for the localization of noncircular sources in near-field.

Data Availability

The data used to support the findings of this study are included within the article.

Conflicts of Interest

The authors declare that there are no conflicts of interest regarding the publication of this paper.

Acknowledgments

This research was supported by the Fundamental Research Funds for the Universities (No. BDY06) and Innovation Project of Science of Technology Commission of the Central Military Commission (No. ∗∗-H863-∗∗-XJ-001-∗∗-02).

References

[1] H. Krim and M. Viberg, "Two decades of array signal processing research: the parametric approach," *IEEE Signal Processing Magazine*, vol. 13, no. 4, pp. 67–94, 1996.

[2] R. Schmidt, "Multiple emitter location and signal parameter estimation," *IEEE Transactions on Antennas and Propagation*, vol. 34, no. 3, pp. 276–280, 1986.

[3] R. Roy and T. Kailath, "ESPRIT-estimation of signal parameters via rotational invariance techniques," *IEEE Transactions on Acoustics, Speech, and Signal Processing*, vol. 37, no. 7, pp. 984–995, 1989.

[4] Y.-D. Huang and M. Barkat, "Near-field multiple source localization by passive sensor array," *IEEE Transactions on Antennas and Propagation*, vol. 39, no. 7, pp. 968–975, 1991.

[5] R.-N. Challa and S. Shamsunder, "High-order subspace-based algorithms for passive localization of near-field sources," in *Proceedings of the Conference Record of the Twenty-Ninth Asilomar Conference on Signals, Systems and Computers*, vol. 2, pp. 777–781, Pacific Grove, CA, USA, October 1995.

[6] J.-H. Lee, Y. Chen, and C.-C. Yeh, "A covariance approximation method for near-field direction-finding using a uniform linear array," *IEEE Transactions on Signal Processing*, vol. 43, no. 5, pp. 1293–1298, 1995.

[7] H. Noh and C. Lee, "A covariance approximation method for near-field coherent sources localization using uniform linear array," *IEEE Journal of Oceanic Engineering*, vol. 40, no. 1, pp. 187–195, 2015.

[8] E. Grosicki, K. Abed-Meraim, and Y. Yingbo Hua, "A weighted linear prediction method for near-field source localization," *IEEE Transactions on Signal Processing*, vol. 53, no. 10, pp. 3651–3660, 2005.

[9] W. Zhi and M. Y.-W. Chia, "Near-field source localization via symmetric subarrays," *IEEE Signal Processing Letters*, vol. 14, no. 6, pp. 409–412, 2007.

[10] X. Chen, J. Ge, C. Wang, X. Zhang, and Q. Yu, "Noncircular DOA estimation algorithm via propagator method and Euler transformation," in *Proceedings of the 2017 3rd IEEE International Conference on Computer and Communications (ICCC)*, pp. 835–842, Chengdu, China, December 2017.

[11] W. Tan, X. Feng, W. Tan, D. Xie, L. Fan, and J. Li, "Direction finding for non-circular sources based on weighted unitary nuclear norm minimization," in *Proceedings of the 2017 IEEE 17th International Conference on Communication Technology (ICCT)*, pp. 1214–1218, Chengdu, China, October 2017.

[12] J. Xie, H. Tao, X. Rao, and J. Su, "Efficient method of passive localization for near-field noncircular sources," *IEEE Antennas and Wireless Propagation Letters*, vol. 14, pp. 1223–1226, 2015.

[13] J. Xie, J. Su, X. Rao, and H. Tao, "Real-valued localisation algorithm for near-field non-circular sources," *Electronics Letters*, vol. 51, no. 17, pp. 1330-1331, 2015.

[14] H. Chen, W. Wang, and W. Liu, "Joint DOA, range, and polarization estimation for rectilinear sources with a cold array," *IEEE Wireless Communications Letters*, vol. 8, no. 5, pp. 1398–1401, 2019.

[15] B. A. Obeidat, Y. Zhang, and M. G. Amin, "Range and DOA estimation of polarized near-field signals using fourth-order statistics," in *Proceedings of the 2004 IEEE International Conference on Acoustics, Speech, and Signal Processing*, vol. 2, pp. 2–97, Montreal, Canada, May 2004.

[16] Y. Wu, H. Wang, Y. Zhang, and Y. Wang, "Multiple near-field source localisation with uniform circular array," *Electronics Letters*, vol. 49, no. 24, pp. 1509-1510, 2013.

[17] J.-W. Tao, L. Liu, and Z.-Y. Lin, "Joint DOA, range, and polarization estimation in the fresnel region," *IEEE Transactions on Aerospace and Electronic Systems*, vol. 47, no. 4, pp. 2657–2672, 2011.

[18] J. He, M. O. Ahmad, and M. N. S. Swamy, "Near-field localization of partially polarized sources with a cross-dipole array," *IEEE Transactions on Aerospace and Electronic Systems*, vol. 49, no. 2, pp. 857–870, 2013.

[19] Y. Xu, J. Ma, and Z. Liu, "Polarization sensitive PARAFAC beamforming for near-field/far-field signals using co-centered orthogonal loop and dipole pairs," in *Proceedings of the 2013 IEEE China Summit and International Conference on Signal and Information Processing*, pp. 616–620, July 2013.

[20] J. Volakis, *Antenna Engineering Handbook*, McGraw-Hill, New York, NY, USA, 4th edition, 2009.

[21] A. Ferréol, E. Boyer, and P. Larzabal, "Low-cost algorithm for some bearing estimation methods in presence of separable nuisance parameters," *Electronics Letters*, vol. 40, no. 15, pp. 966-967, 2004.